



Deliverable No. 9.4

The integrated DrEye platform for image analysis and visualisation

Grant Agreement No.: 600841
Deliverable No.: D9.4
Deliverable Name: The integrated DrEye platform for image analysis and visualisation
Contractual Submission Date: 31/01/2017
Actual Submission Date: 05/05/2017

Dissemination Level		
PU	Public	
PP	Restricted to other programme participants (including the Commission Services)	
RE	Restricted to a group specified by the consortium (including the Commission Services)	X
CO	Confidential, only for members of the consortium (including the Commission Services)	



COVER AND CONTROL PAGE OF DOCUMENT

Project Acronym:	CHIC
Project Full Name:	Computational Horizons In Cancer (CHIC): Developing Meta- and Hyper-Multiscale Models and Repositories for In Silico Oncology
Deliverable No.:	D9.4
Document name:	The integrated DrEye platform for image analysis and visualisation
Nature (R, P, D, O) ¹	P
Dissemination Level (PU, PP, RE, CO) ²	RE
Version:	1
Actual Submission Date:	05/05/2017
Editor: Institution: E-Mail:	Ioannis Karatzanis FORTH karatzan@ics.forth.gr

ABSTRACT:

This deliverable summarizes the main advances in the integrated medical image analysis tools for CHIC within the context of Task 9.5, titled 'An integrated image processing toolkit for CHIC', which runs from M6-M46. The deliverable consists of two parts. In the first part, there is a report on the new functionalities on the DrEye platform, an overview of their use in the segmentation of the DICOM images as performed in the clinical workflow and their use in the transformation of the imaging data, to prepare them for the hypermodels. The second part presents the DrEye, as the integrated imaging platform of CHIC, its interconnection with the visualization tool called CCGVis, the pre-processing tool and the developed Longitudinal Study module.

KEYWORD LIST:

Medical Image analysis, MRI analysis, Segmentation, Medical visualization, DoctorEye, DrEye, Image Processing, MRI, CT, PET, Multi-modal, DCE, biomarkers

¹ R=Report, P=Prototype, D=Demonstrator, O=Other

² PU=Public, PP=Restricted to other programme participants (including the Commission Services), RE=Restricted to a group specified by the consortium (including the Commission Services), CO=Confidential, only for members of the consortium (including the Commission Services)

The research leading to these results has received funding from the European Community's Seventh Framework Programme (FP7/2007-2013) under grant agreement n° 600841.

The author is solely responsible for its content, it does not represent the opinion of the European Community and the Community is not responsible for any use that might be made of data appearing therein.

MODIFICATION CONTROL			
Version	Date	Status	Author
0.1	25/01/2017	Draft	Ioannis Karatzanis
0.8.	31/01/2017	Draft	Ioannis Karatzanis
1.0	30/03/2017	Final	Ioannis Karatzanis

List of contributors

- Ioannis Karatzanis, FORTH
- Stelios Sfakianakis, FORTH
- Norbert Graf, USAAR
- Kostas Marias, FORTH
- Manolis Tsiknakis, TEI-C
- Lefteris Kontopodis, FORTH
- Katerina Nikiforaki, FORTH
- Nigel McFarlane, University of Bedfordshire

Contents

1 Executive Summary	6
2 Introduction	7
2.1 Purpose of this document	7
2.2 Structure of the Deliverable	7
3 DrEye platform	8
3.1 Introduction	8
3.2 Features	8
3.3 System architecture and Integration Platform	9
3.4 Annotation, Segmentation and Visualization	11
3.4.1 Annotation Functionalities	11
3.4.1.1 Generic Anatomy Colors	11
3.4.2 Segmentation Tools	11
3.4.2.1 Magic Wand tool	12
3.4.2.2 Spatially Adaptive Active Contour tool	12
3.4.2.3 Boolean Operations	14
3.5 Visualization	15
3.6 Segmentation of tumours using DrEye	16
3.7 Storing & Sharing of segmentations	17
4 Pre-Processing Tool	19
5 Module for longitudinal analysis	21
5.1 Introduction	21
5.2 Integration and Interaction with DrEye	21
6 Integration with CCGVis	23
6.1 Introduction	23
6.2 Integration and Interaction with DrEye	24
6.2.1 Valid flags	24
6.2.2 Valid format strings	24
6.2.3 Valid task strings	24
6.3 CCGVis Output	25
7 Conclusion	26
8 References	27
Appendix 1 – Abbreviations and acronyms	28
Appendix 2 – Generic Anatomy Colors	29

1 Executive Summary

The main objective of the CHIC project is to offer a computational platform for the biomedical researchers and computational biologists to build complex integrative models which address the challenges in cancer research and treatment using a multilevel and multiscale approach. At the same time, the findings and outcomes of this research in the CHIC computational environment is of high relevance to the needs in the clinical practice and decision support in the clinical setting. Common and fundamental element among the research and the clinical practise is data. Clinical data is the starting point for everything and part of them is the imaging data.

This document aims to describe the developments in the process of creating a unified imaging platform, which deals with the analysis and the display of the imaging data in a one stop shop for both the clinicians and the researchers. During the integration process, there was an effort to provide a seamless experience to the end user, even if in the background different interconnection mechanisms were used among the applications. The tools of the platform assist the clinician to segment the regions of interest (tumours, organs, etc.) using manual or semi-automatic functions, and at the same time there are tools that provide the means for researchers to convert the segmentations in input suitable for use by their models.

2 Introduction

2.1 Purpose of this document

The main purpose of this deliverable is to present an overview of the main DrEye platform's functionalities and in special to report the new features which were implemented in the CHIC context in order to: segment the medical images, process the imaging data in order to be suitable to be used as input to the hyper-models, interconnect with the visualization applications of the WP9 and finally provide feedback based on longitudinal data for the evolution of the disease.

2.2 Structure of the Deliverable

The document is organized as follows:

- Section 3 provides a short description of the DrEye platform, which was first developed in the ContraCancrum project and has been therefore enhanced within CHIC. The section continues with a report on the updates of the platform in order to successfully fulfil its role in the CHIC project and it concludes with the description of a typical tumour delineation as performed by the experts using the tools.
- Section 4 describes the Pre-Processing tool.
- Section 5 describes the Longitudinal Study module.
- Section 6 describes the interconnection with the CCGVis visualization application.
- Section 7 concludes.

3 DrEye platform

3.1 Introduction

The DrEye imaging platform developed in the ContraCancrum [1]. project: DrEye is an open access, flexible and easy to use clinical image analysis and simulation platform, for intuitive annotation and segmentation of tumor regions. Its clinically driven design and development is coupled with an open modular architecture focusing on plug-in components. DrEye's main advantage is that the user can quickly and accurately delineate complex areas in multi-modal medical images that can be loaded simultaneously, while multiple labels can be set to allow the user to annotate and manage many different areas of interest in each selected slide. The close collaboration with clinicians in designing the platform has ensured that it can be effectively used in the clinical setting. Another reported feature that adds value to the platform is that it allows computational "in-silico" models of cancer growth and simulation of therapy response to be easily plugged in, in order to provide a future integrated platform for modelling-assisted therapy decision making. The platform also offers comparison tools for assessing the accuracy of simulations via comparison with the actual therapy outcome. DrEye platform is based on the .NET framework architecture and can be used in any Windows-based computer. The graphical interface is based on well-known Microsoft Office applications to ensure a user-friendly environment.

3.2 Features

- Support for multiple users (with roles and access management)
- View a single DICOM image or a whole series of DICOM images
- View other medical image formats like Meta-Images (mha, mhd+raw) or most other file formats common in the medical imaging field
- Tab interface that allows for multiple series to be opened at once. The interface is easily adjustable to provide side by side views of two or more image modalities.
- Configuration of DICOM Level and Width
- Intuitive navigation/viewing capabilities
- Support for multiple annotations per DICOM image that feature: Label, Color, Types, Opacity,
- Support for Annotation management (merge, sort, ...) and batch editing (rename all, ...)
- Powerful annotation tools: Pen, Eraser, Rectangular Marquee, Elliptical Marquee, Boolean operations among ROIs, Magic Wand, Active contours using Greedy algorithm, Active contours using Snakes algorithm, Semi-automatic selection of outer boundaries, and more...
- Metrics (Ruler, Surface estimation and Volume estimation of a selected ROI/VOI)
- Histogram generation for multiple ROIs
- Plugin Mechanism: More features/functionalities can be added with 3rd party plugins, that can be embedded in the platform seamlessly. SDK and guides are available.
- Import/Export in various common formats (Meta-Image, comma separated csv files, excel files, text files, xml, pdf...)
- A dedicated module for longitudinal analysis that assists the quantitative evaluation of therapy response, through temporal multi-modal imaging examinations and extracted biomarkers.
- Embedded Viewer for DICOM tags
- 3D visualization of a selected series and of its annotations.

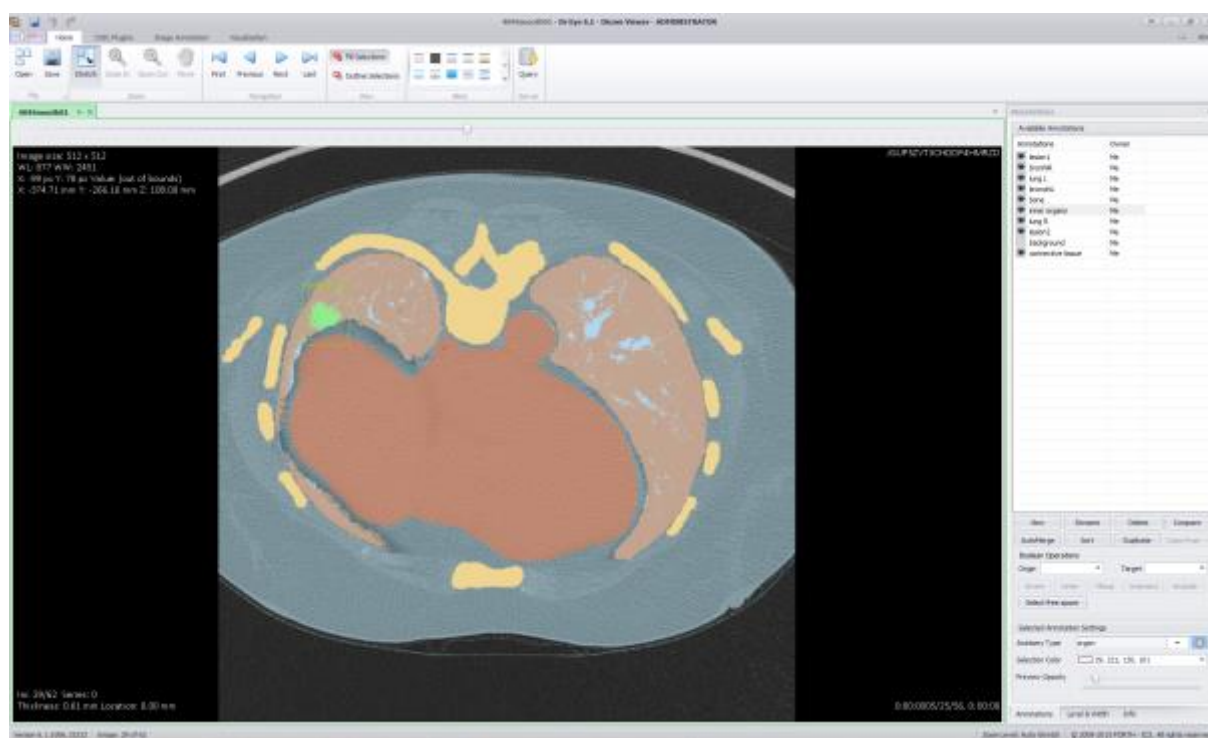


Figure 1 - The main window of the DrEye platform with an MRI data set and annotations

3.3 System architecture and Integration Platform

A high-level block diagram of the system architecture is illustrated in figure 2. The platform is built on three fundamental modules. The "Core Module", the "Plug-in Module" and the "3D Visualization Module". The Core Module represents the basic functionality of the platform which includes an intuitive graphical user interface, tools for primarily handling and processing multi-modal DICOM images (but also other types of medical images such as Meta-Images, Nrrd, etc), tools for creating and managing multi-layered annotations and a variety of built in methods (necessary for the platform's functionality). The Plug-in Module supports platforms' unique extensibility features, rendering it as the solid foundation for algorithms development, either in house (Core available plugins) or from third party developers (third party plugins). Finally, the 3D Visualization module is based on the Visualization Toolkit (VTK), which provides 3D reconstruction and visualization of the annotations and simulations provided by the aforementioned modules.

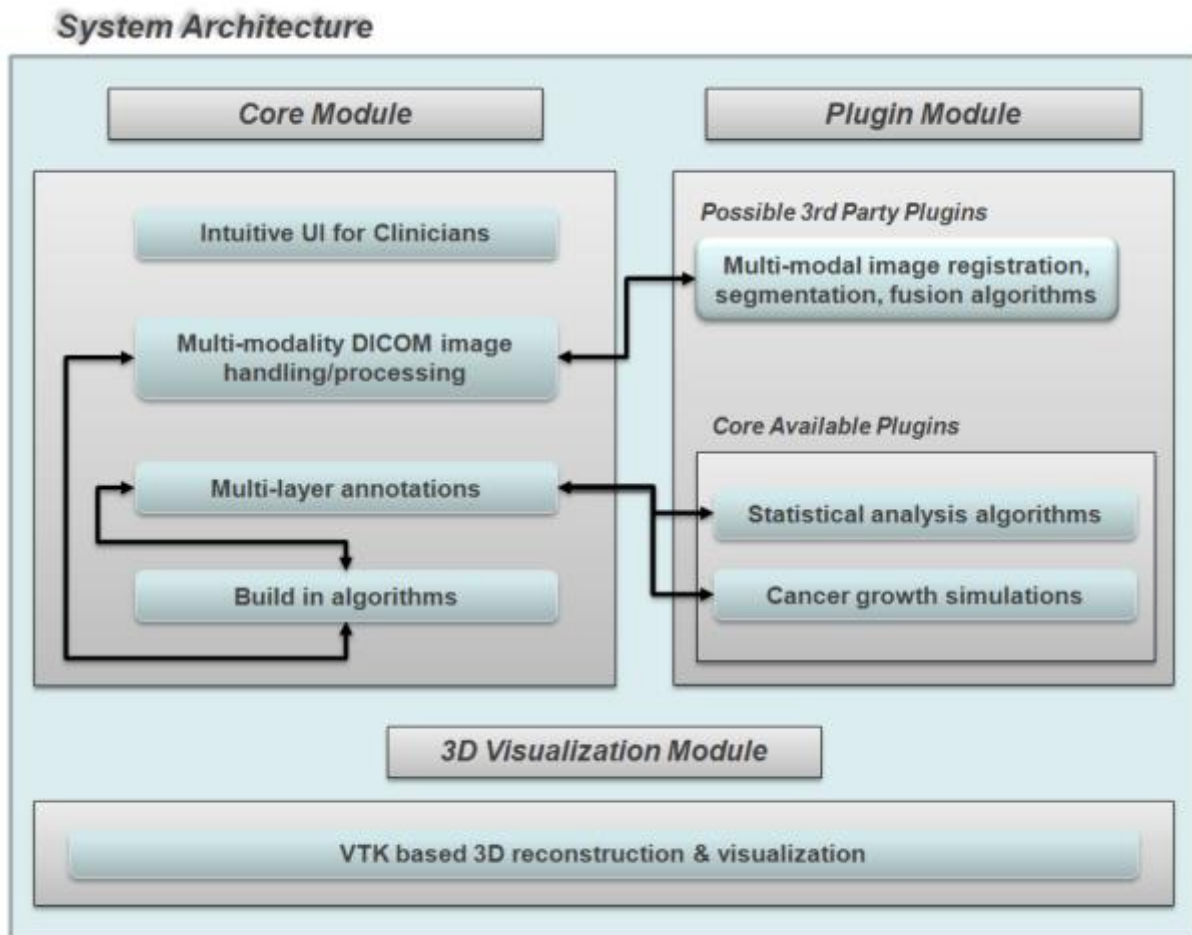


Figure 2 - Block diagram of system architecture.
The three basic modules (Core, Plug-in, 3D Visualization) can be identified.

3.4 Annotation, Segmentation and Visualization

3.4.1 Annotation Functionalities

DrEye provides a powerful annotation mechanism and a series of specialized tools that offer the ability to markup an image without changing the original image data. The annotation panel (Figure 3) shows all the available annotations of a DICOM series in a list. Using the checkboxes, the clinician can toggle the visibility of the annotations. A series of control buttons below the annotation list provide to the clinicians the ability to create and handle annotations and configure their properties (opacity, color).

3.4.1.1 Generic Anatomy Colors

A new feature introduced in the DrEye platform in the context of the CHIC project, is the support for a list of whole body anatomy labels. The Generic Anatomy Colors (GAC)[2] lookup table is a flexible color table for editing medical image data with no prior knowledge of the condition, modality or specific anatomical region being displayed. The table associates integer labels with a respective string that defines an anatomical structure and a representative color in RGB format. GAC also provides a mapping to SNOMED terminology.

The version of the table used in the platform can be found in Appendix 2.

The clinician may associate each annotation with a corresponding anatomical label from the GAC lookup table, simply by selecting an option from the "Anatomy Type" dropdown (Figure 3). In that case, the selected color for the annotation will change to the one associated to the selected structure in the GAC table.

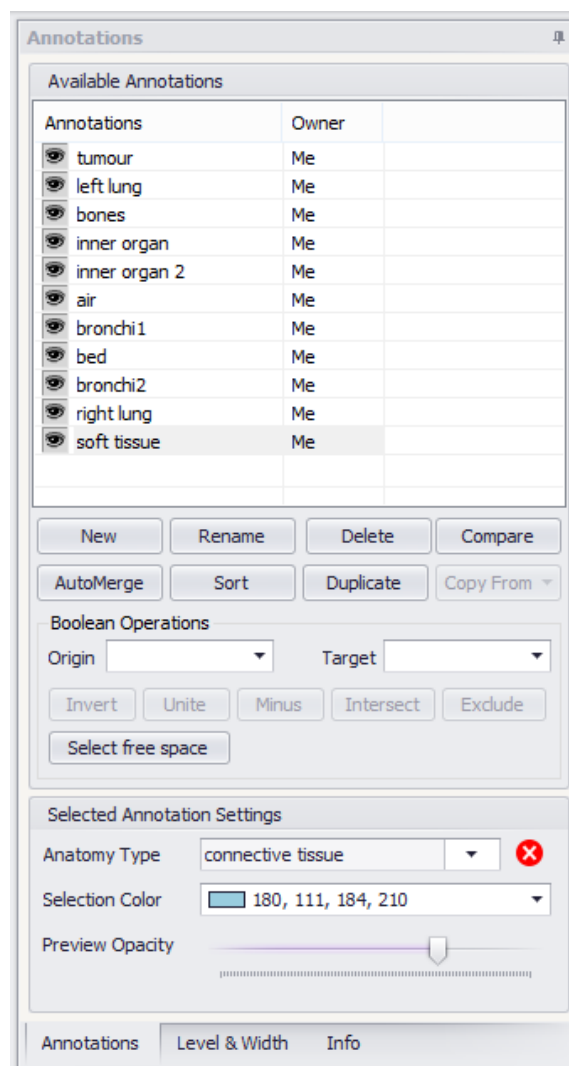


Figure 3 - The annotation panel shows all the available annotations of a DICOM image in a list. Using the checkboxes, the clinician can toggle the visibility of the annotations. A series of control buttons below the annotation list provide to the clinicians the ability to create and handle annotations and configure their properties (opacity, type, color).

3.4.2 Segmentation Tools

All the segmentation tools, are gathered in the "Image Annotation" tab of the top ribbon. The tools

are divided in two groups. The group "Tools" contains tools for manual segmentation, while the group "Algorithms" contains semi-automatic segmentation tools, as shown in Figure 4

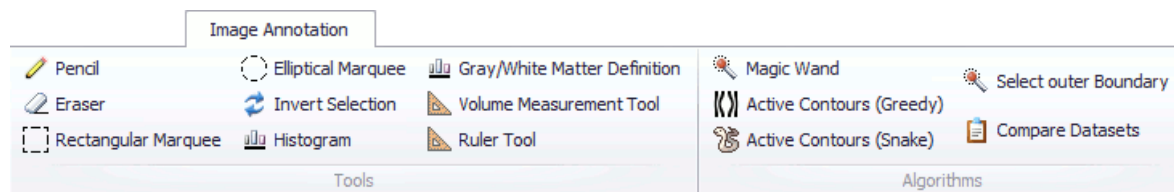


Figure 4 - All the segmentation tools, are gathered in the "Image Annotation" tab of the top ribbon. The tools are divided in two groups. The group "Tools" contains tools for manual segmentation, while the group "Algorithms" contains semi-automatic segmentation tools.

The semi-automatic segmentation tools help the clinicians to perform lightning fast segmentations of areas of interest. A brief description of the functionality of these tools follows:

- The Magic Wand tool selects an area of an image based on similarities between the intensity of the voxels.
- The Greedy Active Contours tool is the default implementation of the active contours algorithm.
- The "Active Contours (Snake)" tool (snake tool) is an innovative approach of the active contours algorithm, performing exceptionally in brain tumor segmentations.

Among these methods a short description follows for the Magic Wand and the Snake tool as they are the ones that are used the most.

3.4.2.1 Magic Wand tool

The Magic Wand tool is based on the Flood fill algorithm (known also as seed fill algorithm), that finds and selects all the connected voxels around a user-selected initial node (point) that are similar in grey intensity (Marias K et al. (2010)[9]). A tolerance value can be specified by the user to determine how closely to match intensities (higher tolerance ends up in a larger selection). The selection can be restricted from boundary conditions set by a user defined rectangle (the working area).

All the points selected by the algorithm are automatically stored in an image mask of the same size as the original image. Each pixel in the image mask represents the position of the selected pixels in the original image and is used to label the delineated tumors. Moreover, to enhance its effectiveness, we implemented a faster version of this algorithm which excludes all the pixels that have already been examined, to ensure that the algorithm does not check them again.

The functionality of the tool is greatly enhanced when used in conjunction with other ROIs using Boolean operations (e.g. from a selected area remove the area defined from the magic wand).

3.4.2.2 Spatially Adaptive Active Contour tool

The Spatially Adaptive Active Contour technique reported in the frames of the World Congress on Medical Physics and Biomedical Engineering [4], is an extension on the traditional active contours, or snakes, which have been widely used in image processing for segmenting image entities and delineate object boundaries. The snake algorithm, first introduced by Kass et al. [5], is a

semiautomatic method, based on the deformation of an initial contour towards the boundary of the desired object, which is accomplished by trying to minimize energy functional, and designed so that its minimum is obtained at the desired boundary. The snake evolution can be driven by adjusting four constant and global parameters, which control the curve's smoothness and continuity, and the force that pushes the snake to expand.

In the platform described in this paper we integrated an improved version of the traditional active contours, which Marias K. et al. (2010) call the Spatially Adaptive Active Contours [10]. This algorithm is based on the discrimination of image regions according to underlying characteristics, such as gradient magnitude and corner strength, and the assignation to each region with a different "localized" set of parameters, one corresponding to a very flexible snake, and the other corresponding to a very rigid one, according to the local image features. Therefore, the snake exhibits different behaviour within image regions with diverse characteristics, thus, providing more accurate boundary delineation.

This segmentation technique is semi-automatic, which means that the user only needs to place an initial contour inside the desired object (tumour area or organ) and let it evolve towards its boundaries. It has been extensively tested on real data of Wims' tumour cases and seems to follow very satisfyingly the clinical expert's intuition, concerning the true tumour boundaries.

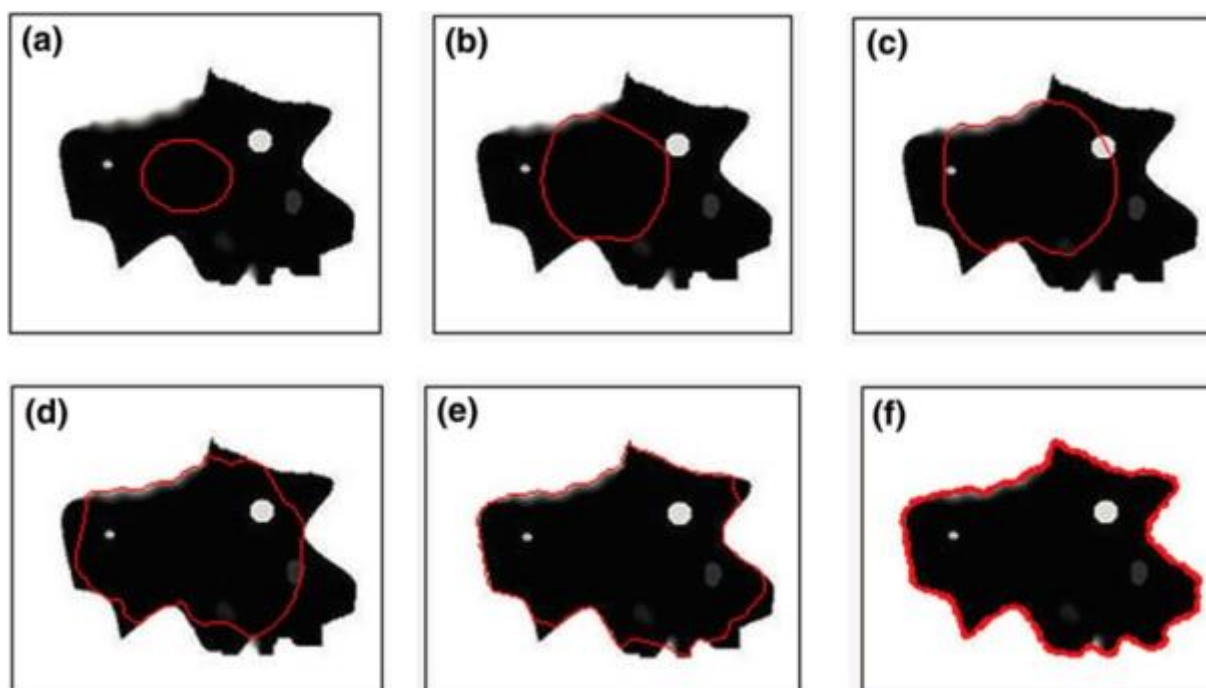


Figure 5 - (a - e) Snake deformation in progress, using the spatially adaptive active contour algorithm, (f) final result.

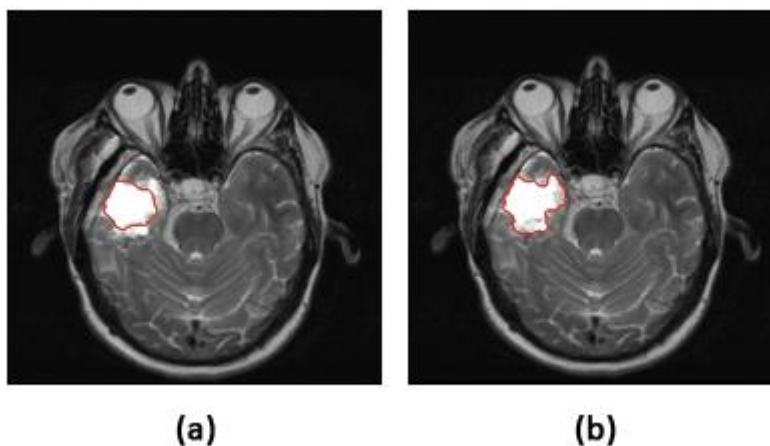


Figure 6- Example of the application of the traditional snakes, as well as the improved active contours approach on a real brain image. It is obvious that the spatially adaptive snake (b) intuitively follows the true tumor outline, while the traditional snake (a) is caught up in the small inhomogeneities inside of the tumor.

3.4.2.3 Boolean Operations

To allow for more complex segmentations, two segmentations can be combined together into a compound segmentation, on which Boolean operations can be set. These are accessible in the "Boolean Operations" section of the Annotations panel (Figure 7) and include: Union (+), Minus (–), Intersect and Exclude (Figure 8). This is a new feature in order to facilitate the experts and reduce the time of the segmentation process.

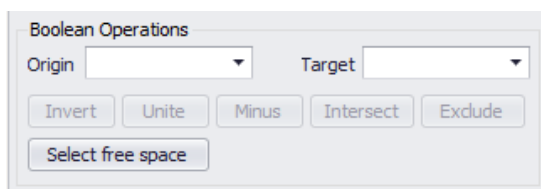


Figure 7 - The Boolean Operations controls

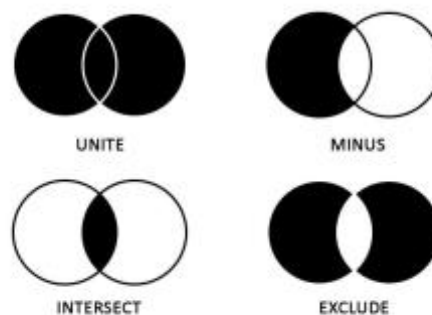


Figure 8 - Supported Boolean operations

3.5 Visualization

DrEye provides a visualization tool, in the form of a native plugin, for reconstructing the two-dimensional DICOM images to three-dimensional volumes. The plugin is built upon the Visualization Toolkit (VTK) and it provides 3D visualization of the dataset slices and 3D rendering of the segmented volumes. The 3D Visualization plugin is an interactive three-dimensional viewer which offers user freedom of interaction with the imaging data in 3D (rotate camera angle, zoom in/out, pan etc), and also a basic set of configuration options (color mapping/ opacity setting/ visibility switching of the DICOM slides or the segmentation volumes/ clipping plane, etc.).

As the 3D visualization capabilities of the DrEye platform are specialized for DICOM datasets and their segmentations, the need to visualize complex and multiple outputs of varied file formats is handled by the proper advanced tool, the CCGVis. CCGVis supports the visualization and comparison of both medical and simulation data. More information on the CCGVis and its integration with DrEye is in section 6 of this document.

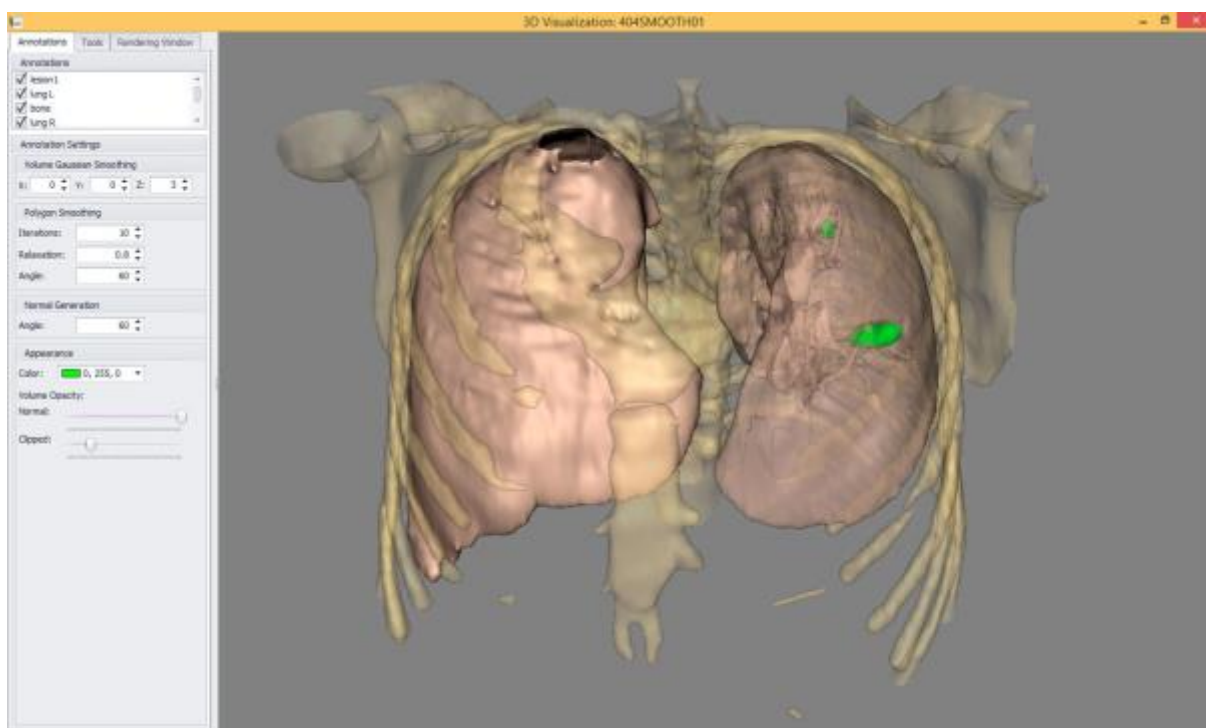


Figure 9 - 3D visualization of a non small lung cancer patient using the 3D visualization tool of DrEye, with lower opacities for the bones and the left lung in order to see the tumors (green color)

3.6 Segmentation of tumours using DrEye

Tumour images segmentation activities in general are very complex due to high variability of tumour structures. Since manual segmentation is time-consuming, and, on the other side, a fully automatic technique is not applicable because the enrolment of the clinician's expertise/supervision is required, the best choice seems to be a semi-automatic technique with usually minor manual corrections (if necessary).

Longitudinal imaging data from patients diagnosed with non-small lung cancer, neuroblastoma or glioblastoma were included in the database. Clinical information on the dates of specific therapeutic interventions was also available in order to evaluate disease progression from consecutive examinations. In the following paragraphs of this section the typical segmentation and processing workflow will be described for the non-small lung cancer cases. The workflow is analogous in the rest cancer types.

For each time point, functional (PET) and anatomical (CT) images were superimposed in order to delineate the area of abnormal functional activity (named as "lesion") on the anatomy. A solid mass in the lung parenchyma with PET activation was considered as active disease. The corresponding tissue was located on the CT DICOM data and the precise tumor outline was defined by user supervised semi-automated analysis, based on pixels within a specific range of Hounsfield units. Because of the different spatial resolution of the two methods, the area of interest was not copied automatically, but it was manually done by the user by viewing the DICOM files side by side. Several functionalities facilitated the segmentation process, such as the magic wand, the definition of a working area, the boolean operations as well as the more conventional pencil and eraser with variable size. Where available, this procedure was repeated at a later time point in order to evaluate changes in tumor size, after treatment or disease progression.

In the second laborious step of healthy tissue segmentation new features were necessary in order to avoid having unassigned pixels or pixels belonging to two or more different neighbouring entities. Such features are automatic marking of the non segmented pixels as "free area", excluding pixels that have already been assigned to an existing annotation and ROI dilatation or erosion in order to improve ROI delineation. The added possibility to save / import the segmentation as a XML or Meta-Image file reduced the complexity in the final step of data storing or sharing as the segmentation can be separated from the DICOM folder.

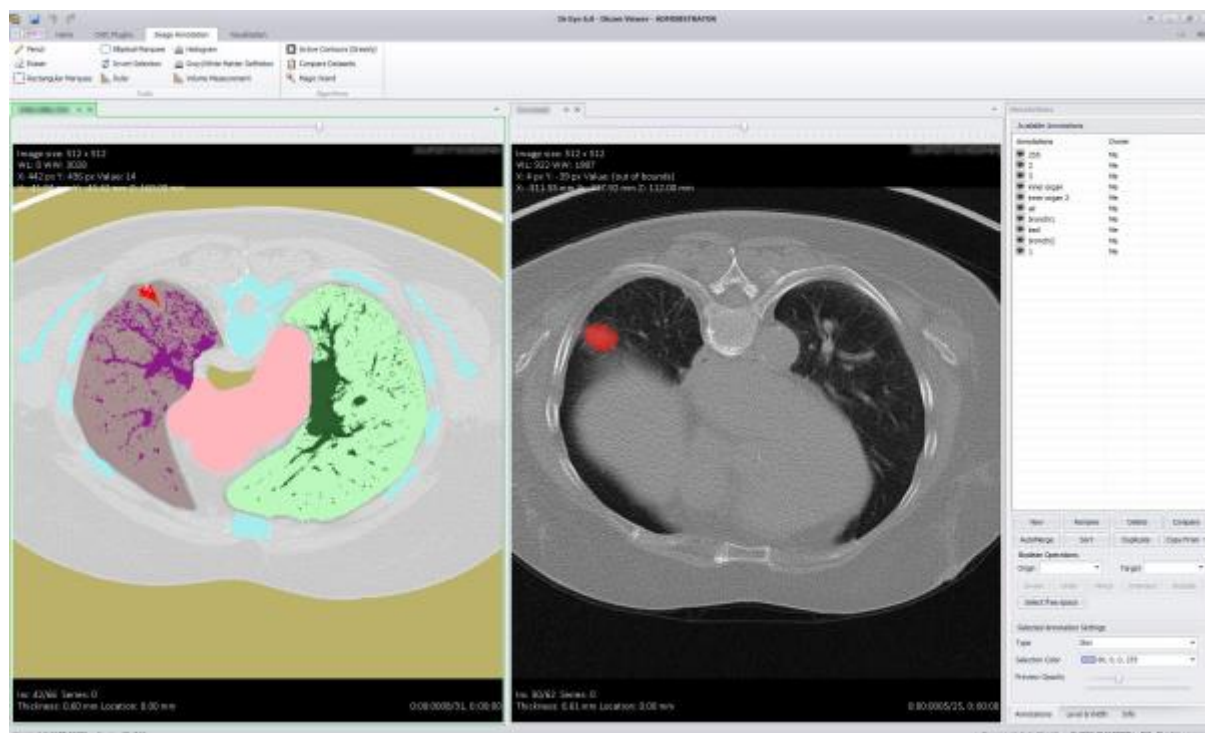


Figure 10 - Side by side overview of two different time points

3.7 Storing & Sharing of segmentations

Segmentations performed by experts using DrEye, can be saved in various ways. The default way of storing in DrEye is to save the segmentations inside the DICOM file, in a way that does not alter the image data. In detail the pixel data remain untouched and all the information is stored as XML data in a specific tag (not proprietary/private) intended to hold supplementary textual information. The pros in that the segmentations are bundled together with the imaging data are that there is no need to have a linking mechanism with the original data (it copes with the risk of potential separation or wrong linking), that the DICOM files remain readable by any other viewer (although the annotations probably will not show) and that it is usually easy to share as you just exchange the files. The cons are that this method is not widely adopted and this makes sharing to other tools very difficult. Therefore, many alternative export options are provided in the DrEye platform, in order to facilitate the clinicians (or other stakeholders) and make attractive the use of the platform in heterogeneous workflows. Supported export options in DrEye are Meta-Image, xml, comma separated (csv), excel, text, pdf, with the most common for the segmentations the xml and the Meta-Image.

In the context of CHIC, the selected file format used for the segmentations is the Meta-Image, in its single file (mha) form, as it is a standard format, widely adopted by many applications. It is also fully anonymised as it only contains imaging information (without any patient data). The segmentations are uploaded to the CDR which keeps a link to the associated DICOM series.

The Insight Segmentation and Registration Toolkit (ITK) is a widespread image processing library. ITK's native file format is the Meta-Image, that has either .mha or .mhd file extension. In a Meta-Image the data are raw and uncompressed. The only difference between mha and mhd is that mha contains header and image data in same file, while mhd is comprised by two files, a .raw file which stores the image data and a .mhd file which stores only the header and a link to the .raw file. The separation of the header from the raw data in discrete files, makes the mhd readable by simple text

readers.

4 Pre-Processing Tool

As described in section 3.6 (Storing & Sharing of segmentations), segmentations that were delineated in DrEye are exported in a single file Meta-Image (having a .mha file extension). That Meta-Image contains all the anatomical structures and it inherits all the grid properties (spacing between voxels, width and height, etc.) from the original DICOM series. It is also the one that is uploaded in the CDR, where is associated with the corresponding DICOM series, and is available to be used as input to the models.

The OncoSimulator though requires as input a Meta-Image that contain no other anatomy except of the tumor (with configurable spacing around and redefined tumor label value), and on top of that it should be isotropic (same node spacing in any direction of the grid). Another requirement is that the volume properties (width, length, height, and grid spacing) must be contained in a text file, in order to be easily read, and that is the case of a Meta-Image with a separate header (mhd file format). The latter Meta-Image consists of two files, a header file (mhd file extension) which contains the volume properties in a textual format, and a binary file with the raw data (raw file extension).

The Pre-Processing tool has its own important key role at the CHIC platform, as it converts the multi-labelled segmentation Meta-Image retrieved from the CDR (containing all the anatomical structures) to a Meta-Image that contains only tumor information and it is properly formatted in order to be suitable input for the OncoSimulator. The conversion in short performs the following operations at the Meta-Image with the segmentations: filtering of the anatomy labels to keep only the tumor, relabelling of the tumor value (tumor is represented as mass in the GAC list with value 7, while the OncoSimulator uses a mask where the tumor voxels have value 255), resampling of the space and then cropping using a threshold to provide enough spacing for the tumour growth.

There are two editions of the tool, a command line executable program and a plugin in DrEye. The command line edition has been developed in python using the Insight Segmentation and Registration Toolkit (ITK), and it is used behind the scenes in the CHIC platform in order to transform appropriately the Meta-Images, as described above. The edition which is bundled in DrEye has been developed in C# using again the ITK library. At the table below, there are the command line arguments of the Pre-Processing tool, and their description. The options remain the same for the DrEye's edition of the tool.

The tool accepts the following command line arguments:

Argument	Required	Description
-i {input_file}	Yes	Path to a valid Meta-Image (mha format), which contains the segmentations with the tumor value to be 255.
-o {output_file}	Yes	Path to save the interpolated and cropped result.
-t {threshold}	No	The threshold for the cropping (float between 0 and 1). If omitted 0.3 is used (=30%).
-r {interpolation spacing}	No	The spacing to be used for the isotropic interpolation. If omitted 1.0 is used.

Table 1 - Table of Input arguments of the Pre-Processing tool.

5 Module for longitudinal analysis

5.1 Introduction

The longitudinal study module [11] has been developed for the purposes of the CHIC Project and has been tested with real data to support hypothesis driven research from the oncologists of the project. The purpose of this module is on one hand to assist the quantitative evaluation of therapy response through temporal multi-modal imaging examinations and extracted biomarkers (e.g. DCE MRI), and on the other hand, to enable effective comparison between actual patient outcome data and predictions in order to validate cancer models.

Beyond the conventional MR imaging, where anatomical information can be extracted from the imaging data, there are also advanced protocols that allow the quantification of the imaging data. In these cases, sequential 3D volumes are acquired by changing an imaging parameter such as image acquisition timing (before, during and after the intravenous administration of a paramagnetic contrast agent in DCE-MRI) or diffusion weighting value (sequential diffusion weighted acquisitions by changing the b-value parameter in DW-MRI). The resulted 4D imaging data can be evaluated either by visual inspection from an expert radiologist or by fitting the resulted 4D data to a mathematical model that describes the underlying procedure. The former is simple and easy to be performed, however it is user dependent and does not provide quantifiable markers that can be further processed and used in comparative studies. The quantification procedure will provide per voxel parametric maps of the model biomarkers that can be stored as medical images (e.g. DICOM) and transferred to relevant software tools for further evaluation.

5.2 Integration and Interaction with DrEye

To this end, a visualization module has been implemented and incorporated in the DrEye platform facilitating the workflow in follow up studies and giving the end user the option to detect and quantify differences in the temporal evolution of the imaging features.

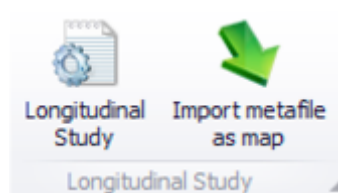


Figure 11 - The section of the "CHIC plugins" tab (at the main ribbon toolbar) that contains the functionalities of the module for longitudinal analysis.

The end user can compare side by side datasets from longitudinal studies or cohort based exams through an intuitive user interface. There is also the option to compare either the raw MRI data or the biomarkers extracted through perfusion and diffusion quantitative models superimposed on the anatomical and functional raw images, and finally compare the automatically calculated histograms of the ROIs delineated by the user. Statistical measurements (mean, standard deviation, skewness, kurtosis, etc.) that have been frequently used in quantitative analysis for diagnosis, therapy assessment, grading and classification of different tumor types [6] [7] can be also computed automatically in these regions. Finally, the clinician can export the information visualized in DrEye in a pdf report. Other imaging modalities, such as PET and CT, can also be supported by the aforementioned longitudinal analysis module but have not been tested yet.

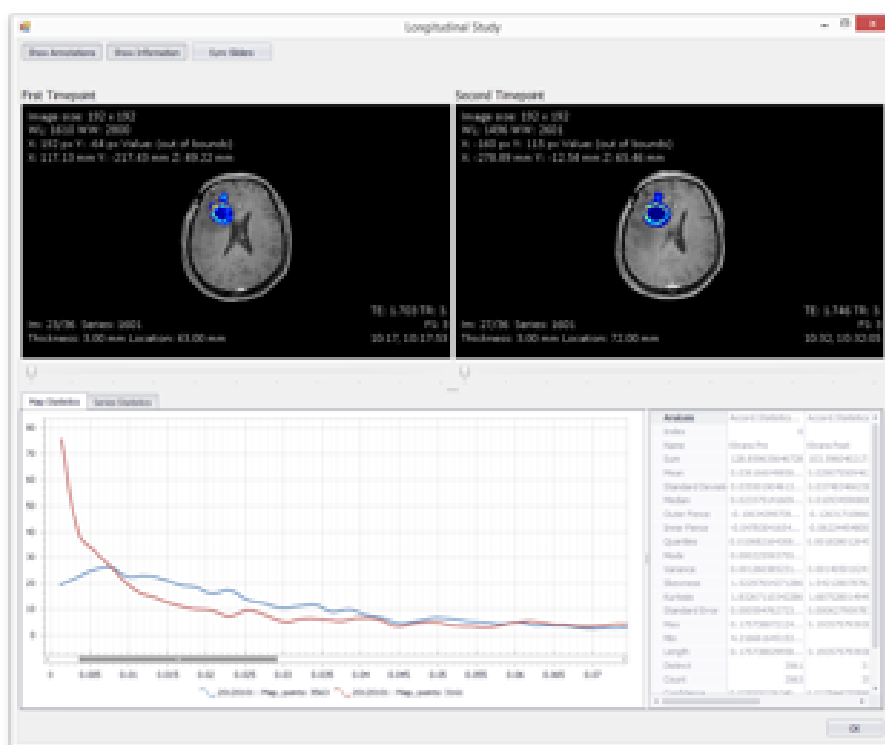


Figure 12 - In the upper part of the figure, there is depicted the side by side comparison of the ktrans maps over the DICOM slides, while in the lower part there is the overview of the histograms & statistic magnitudes for the corresponding ROIs [6]

6 Integration with CCGVis

6.1 Introduction

CCGVis is a desktop tool for visualizing and comparing tumours and simulations. CCGVis can import, register and visualize medical data, segmentation data and simulations. It can import various formats, including dicom, mha, nifti and CHIC simulations. Images can be imported singly, in image/segmentation pairs, or as time series. Metadata containing information about the segmentation labelling and the image projection can be added in the form of json files. Visualizations include slice and orthoslice views in 2D and 3D, isosurfaces in 3D, volume rendering, comparisons between real and simulated tumours, and plots of tumour growth. Images and video can be saved to file with captions for later reporting. CCGVis can be executed as a standalone desktop application, or it can be launched from another application with command-line arguments. Input and output data is exchanged via the local file system, in directories specified by the command line arguments.

The API consists of a display window, a widget panel for interactive control, and menus for loading data and launching visualization tasks.

Detailed information regarding CCGVis and its technologies can be found in the deliverable 9.2 A Model and Data Visualization Toolkit. In this document we focus solely to its usage and interconnection with DrEye.

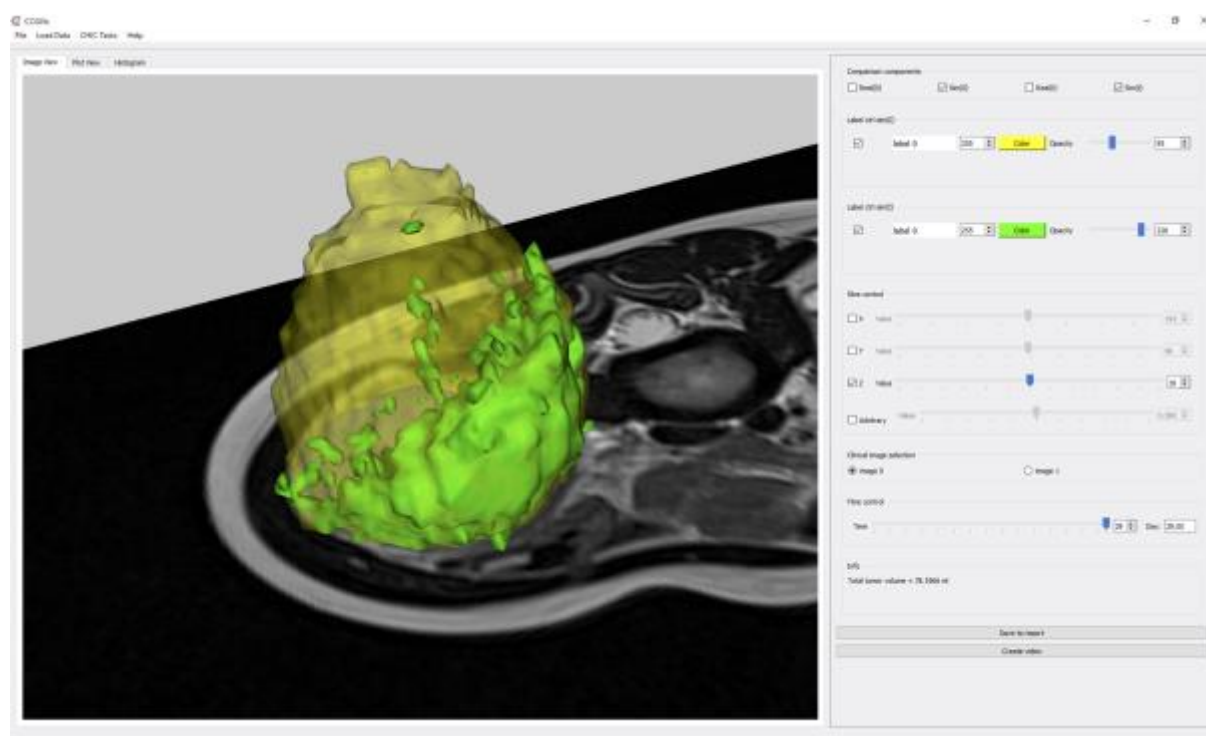


Figure 13 - 3D superimposed comparison visualization of nephroblastoma, showing baseline simulated tumour at day 0 (yellow) with simulated tumour at day 29 (green).

6.2 Integration and Interaction with DrEye

CCGVis can accept command line arguments, through which offers the ability to preload data and to launch tasks on execution. This allows CCGVis to be launched from a batch file or from another program. The latter is the use case in DrEye. In DrEye a plugin has been created to allow the usage of CCGVis in just a click (from the button CCGVis, at the visualization section of the CHIC toolbar). Upon launch DrEye creates a separate process for the CCGVis, controlling its inputs and monitoring its output. The plugin passes all the necessary information from DrEye to CCGVis, using the command line arguments interface.

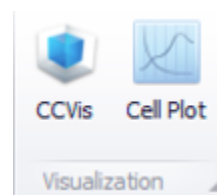


Figure 14

Command line flags are also available for setting the input and output directories.

6.2.1 Valid flags

--Scenario:	“Lung”, “Nephroblastoma”, “Prostate”, “Glioblastoma”. Not currently used.
--Dataset:	Starts a new dataset.
--Format str:	specifies format of dataset.
--ImageSegPair:	(optional) indicates that the following 2 files are a pair: image plus segmentation. A pair counts as one data item with two components.
--TimeSeries n:	(optional) the dataset is a time series containing n items.
--InputDir:	the next item specifies a general default path for input data.
--OutputDir:	the next item is the path where CCGVis will put its output.
--Task str:	specify task to run on launch
--ShowMaximised:	request window maximised on launch
--AutoVideo:	create video output when task is launched without user interaction.

6.2.2 Valid format strings

“Mha”	“DicomDir”	“Nifti”	“ChicSimRaw”
-------	------------	---------	--------------

6.2.3 Valid task strings

"ViewImage2D"	"ViewDicomDir2D"	"ViewImage3D"
"ViewDicomDirOrtho"	"ViewImagePair2D"	"ViewMhaPair2D"
"ViewImagePair3D"	"CompareMhaChicSimOrtho"	"ViewImagePairSeries3D"
"ViewMhaSeries"	"CompareTwoDicomSegmentations3D"	"ViewChicSim"
"CompareMhaChicSim2D"	"CompareMhaChicSimSuperimposed"	"DoNothing"
"ViewMha"	"CompareTwoNiftiSegmentations3D"	

6.3 CCGVis Output

From within CCGVis the "Save to report" button saves an output image of the current image or plot in the main window that can be used in the compilation of the pdf report of the experiment. A caption describing the image is added to a text file. The "Create video" button creates and saves an animated 360° video of a 3D visualization. The outputs are sent to the output directory specified in the command line arguments.

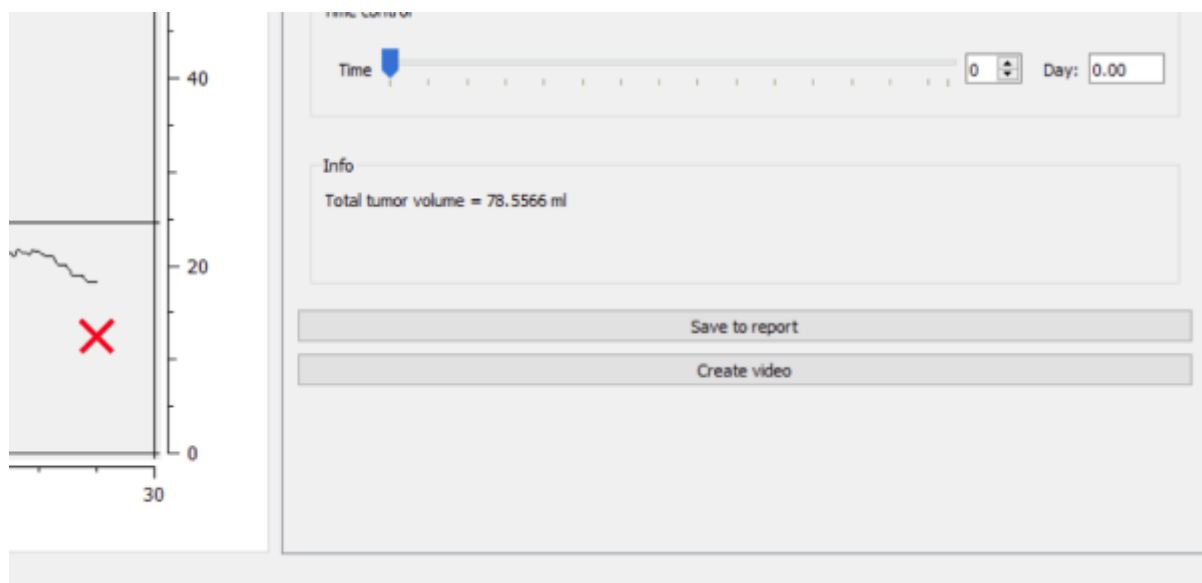


Figure 15 - Snapshot of the CCGVis, showing the buttons from where the images or video can be saved.

7 Conclusion

DrEye fulfils its role as an open access platform that facilitates clinicians and experts to identify any number of distinct 3D features, such as tumors in complex medical images, and annotate them individually. Due to the scalable architecture of the platform it serves as the basis of the integrated DrEye platform for image analysis and visualization, as it successfully merges with CCGVis, the core visualization component of the CHIC project. The platform is expanded with the functionalities of the Longitudinal Analysis module and the Pre-Processing tool, and in conjunction with the new tools (the extra import/export options, the support of the GAC list, etc.) the integrated platform stands out as the one stop shop for image processing tasks in the CHIC context.

DrEye's manual and semi-automatic segmentation techniques, combined with its integrated correction tools, assisted the experts in the quick and refined delineation of tumours and other anatomical structures. The resulted segmentations were processed as needed and converted to the proper input format for the models that required imaging data or the other imaging related information (e.g. segmentations' volume and other statistical information). And finally CCGVis provided great assistance to the clinicians to visualize the data, compare the results and grasp their morphology.

8 References

- [1] ContraCancrum. (n.d.). Retrieved from <http://contracancrum.eu/>
- [2] Halle, M., Talos, F., Kikinis, R., Pieper, S., Aucoin, N., & Jakab, M. (2010). GenericAnatomyColors - SlicerWiki. Retrieved from <https://www.slicer.org/wiki/Documentation/4.6/SlicerApplication/LookupTables/GenericAnatomyColors>
- [3] Skounakis, E., Farmaki, C., Sakkalis, V., Roniotis, A., Banitsas, K., Graf, N., & Marias, K. (2010). DoctorEye: A clinically driven multifunctional platform, for accurate processing of tumors in medical images. *Intelligent Signal and Image Processing in eHealth*, 4.
- [4] Farmaki C, Marias K, Sakkalis V, Graf N. A spatially adaptive active contour method for improving semi-automatic medical image annotation. In: *Proceedings of the World Congress on Medical Physics and Biomedical Engineering 2009*; pp. 1878-81.
- [5] Kass M, Witkin A, Terzopoulos D. Snakes: Active contour models. *Int J Comput Vis* 1987; 1: 321-31.
- [6] E. Kontopodis, G. Kanli, G. C. Manikis, S. Van Cauter, and K. Marias, 2015 “Assessing treatment response through generalized pharmacokinetic modeling of DCE-MRI data, *Cancer Informatics: Computer Simulation, Visualization, and Image Processing of Cancer Data and Processes*”, vol. 14, pp. 41–51.
- [7] X. Li, Y. Zhu, H. Kang, Y. Zhang, H. Liang, S. Wang, and W. Zhang, Glioma grading by microvascular permeability parameters derived from dynamic contrast-enhanced MRI and intratumoral susceptibility signal on susceptibility weighted imaging. 2015. *Cancer Imaging*, vol. 15, p. 4.
- [8] Lorensen, B., Schroeder, W., & Martin, K., VTK - The Visualization Toolkit. Retrieved from <http://www.vtk.org/>
- [9] Skounakis E, Farmaki C, Sakkalis V, Roniotis A, Banitsas K, Graf N, Marias K. DoctorEye: A Clinically Driven Multifunctional Platform, for Accurate Processing of Tumors in Medical Images. *Open Med Inform J*. 2010;4:105-15.
- [10] Farmaki C, Marias K, Sakkalis V, Graf N. Spatially adaptive active contours: a semi-automatic tumor segmentation framework. *Int J Comput Assist Radiol Surg*. 2010 Jul;5(4):369-84.
- [11] Eleftherios, K., Ioannis, K., Vangelis, S., Buffa, F., & Kostas, M. (2016). A DCE-MRI analysis workflow. In *Proceedings of the 33rd Computer Graphics International* (pp. 101–104). ACM.

Appendix 1 – Abbreviations and acronyms

<i>CDR</i>	Clinical Data Repository
<i>SOA</i>	Service Oriented Architecture
<i>GAC</i>	Generic Anatomy Colors
<i>ROI</i>	Region Of Interest
<i>VOI</i>	Volume Of Interest
<i>ITK</i>	Insight Segmentation and Registration Toolkit or just, Insight Toolkit
<i>VTK</i>	Visualization Toolkit
<i>MHA</i>	Meta-Image
<i>MHD</i>	Meta-Image
<i>DrEye</i>	Medical Image analysis platform of FORTH. It is also referred to as DoctorEye.
<i>CCGVis</i>	Advanced 3D visualization application from Centre for Computer Graphics and Visualisation (CCGV) of University of Bedfordshire

Appendix 2 – Generic Anatomy Colors

integer label	text_label	color	notes
0	background	rgba(0,0,0,0)	
1	tissue	rgb(128,174,128)	Default label for bodily tissues
2	bone	rgb(241,214,145)	
3	skin	rgb(177,122,101)	
4	connective tissue	rgb(111,184,210)	
5	blood	rgb(216,101,79)	
6	organ	rgb(221,130,101)	
7	mass	rgb(144,238,144)	Could be tumor or other lesion
8	muscle	rgb(192,104,88)	
9	foreign object	rgb(220,245,20)	Implants, surgical instruments, table...
10	waste	rgb(78,63,0)	
11	teeth	rgb(255,250,220)	
12	fat	rgb(230,220,70)	
13	gray matter	rgb(200,200,235)	
14	white matter	rgb(250,250,210)	
15	nerve	rgb(244,214,49)	
16	vein	rgb(0,151,206)	
17	artery	rgb(216,101,79)	
18	capillary	rgb(183,156,220)	
19	ligament	rgb(183,214,211)	
20	tendon	rgb(152,189,207)	
21	cartilage	rgb(111,184,210)	
22	meniscus	rgb(178,212,242)	

23	lymph node	rgb(68,172,100)	
24	lymphatic vessel	rgb(111,197,131)	
25	cerebro-spinal fluid	rgb(85,188,255)	
26	bile	rgb(0,145,30)	
27	urine	rgb(214,230,130)	
28	feces	rgb(78,63,0)	
29	gas	rgb(218,255,255)	
30	fluid	rgb(170,250,250)	
31	edema	rgb(140,224,228)	
32	bleeding	rgb(188,65,28)	
33	necrosis	rgb(216,191,216)	
34	clot	rgb(145,60,66)	
35	embolism	rgb(150,98,83)	
36	head	rgb(177,122,101)	
37	central nervous system	rgb(244,214,49)	
38	brain	rgb(250,250,225)	
39	gray matter of brain	rgb(200,200,215)	
40	telencephalon	rgb(68,131,98)	
41	cerebral cortex	rgb(128,174,128)	
42	right frontal lobe	rgb(83,146,164)	
43	left frontal lobe	rgb(83,146,164)	
44	right temporal lobe	rgb(162,115,105)	
45	left temporal lobe	rgb(162,115,105)	
46	right parietal lobe	rgb(141,93,137)	
47	left parietal lobe	rgb(141,93,137)	
48	right occipital lobe	rgb(182,166,110)	
49	left occipital lobe	rgb(182,166,110)	
50	right insular lobe	rgb(188,135,166)	
51	left insular lobe	rgb(188,135,166)	

52	right limbic lobe	rgb(154,150,201)	
53	left limbic lobe	rgb(154,150,201)	
54	right striatum	rgb(177,140,190)	
55	left striatum	rgb(177,140,190)	
56	right caudate nucleus	rgb(30,111,85)	
57	left caudate nucleus	rgb(30,111,85)	
58	right putamen	rgb(210,157,166)	
59	left putamen	rgb(210,157,166)	
60	right pallidum	rgb(48,129,126)	
61	left pallidum	rgb(48,129,126)	
62	right amygdaloid complex	rgb(98,153,112)	
63	left amygdaloid complex	rgb(98,153,112)	
64	diencephalon	rgb(69,110,53)	
65	thalamus	rgb(166,113,137)	
66	right thalamus	rgb(122,101,38)	
67	left thalamus	rgb(122,101,38)	
68	pineal gland	rgb(253,135,192)	
69	midbrain	rgb(145,92,109)	
70	substantia nigra	rgb(46,101,131)	
71	right substantia nigra	rgb(0,108,112)	
72	left substantia nigra	rgb(0,108,112)	
73	cerebral white matter	rgb(250,250,225)	
74	right superior longitudinal fasciculus	rgb(127,150,88)	
75	left superior longitudinal fasciculus	rgb(127,150,88)	
76	right inferior longitudinal fasciculus	rgb(159,116,163)	
77	left inferior longitudinal fasciculus	rgb(159,116,163)	

78	right arcuate fasciculus	rgb(125,102,154)	
79	left arcuate fasciculus	rgb(125,102,154)	
80	right uncinate fasciculus	rgb(106,174,155)	
81	left uncinate fasciculus	rgb(106,174,155)	
82	right cingulum bundle	rgb(154,146,83)	
83	left cingulum bundle	rgb(154,146,83)	
84	projection fibers	rgb(126,126,55)	
85	right corticospinal tract	rgb(201,160,133)	
86	left corticospinal tract	rgb(201,160,133)	
87	right optic radiation	rgb(78,152,141)	
88	left optic radiation	rgb(78,152,141)	
89	right medial lemniscus	rgb(174,140,103)	
90	left medial lemniscus	rgb(174,140,103)	
91	right superior cerebellar peduncle	rgb(139,126,177)	
92	left superior cerebellar peduncle	rgb(139,126,177)	
93	right middle cerebellar peduncle	rgb(148,120,72)	
94	left middle cerebellar peduncle	rgb(148,120,72)	
95	right inferior cerebellar peduncle	rgb(186,135,135)	
96	left inferior cerebellar peduncle	rgb(186,135,135)	
97	optic chiasm	rgb(99,106,24)	
98	right optic tract	rgb(156,171,108)	
99	left optic tract	rgb(156,171,108)	
100	right fornix	rgb(64,123,147)	
101	left fornix	rgb(64,123,147)	
102	commissural fibers	rgb(138,95,74)	

103	corpus callosum	rgb(97,113,158)	
104	posterior commissure	rgb(126,161,197)	
105	cerebellar white matter	rgb(194,195,164)	
106	CSF space	rgb(85,188,255)	
107	ventricles of brain	rgb(88,106,215)	
108	right lateral ventricle	rgb(88,106,215)	
109	left lateral ventricle	rgb(88,106,215)	
110	right third ventricle	rgb(88,106,215)	
111	left third ventricle	rgb(88,106,215)	
112	cerebral aqueduct	rgb(88,106,215)	
113	fourth ventricle	rgb(88,106,215)	
114	subarachnoid space	rgb(88,106,215)	
115	spinal cord	rgb(244,214,49)	
116	gray matter of spinal cord	rgb(200,200,215)	
117	white matter of spinal cord	rgb(250,250,225)	
118	endocrine system of brain	rgb(82,174,128)	
119	pituitary gland	rgb(57,157,110)	
120	adenohypophysis	rgb(60,143,83)	
121	neurohypophysis	rgb(92,162,109)	
122	meninges	rgb(255,244,209)	
123	dura mater	rgb(255,244,209)	
124	arachnoid	rgb(255,244,209)	
125	pia mater	rgb(255,244,209)	
126	muscles of head	rgb(201,121,77)	
127	salivary glands	rgb(70,163,117)	
128	lips	rgb(188,91,95)	
129	nose	rgb(177,122,101)	

130	tongue	rgb(166,84,94)	
131	soft palate	rgb(182,105,107)	
132	right inner ear	rgb(229,147,118)	
133	left inner ear	rgb(229,147,118)	
134	right external ear	rgb(174,122,90)	
135	left external ear	rgb(174,122,90)	
136	right middle ear	rgb(201,112,73)	
137	left middle ear	rgb(201,112,73)	
138	right eyeball	rgb(194,142,0)	
139	left eyeball	rgb(194,142,0)	
140	skull	rgb(241,213,144)	
141	right frontal bone	rgb(203,179,77)	
142	left frontal bone	rgb(203,179,77)	
143	right parietal bone	rgb(229,204,109)	
144	left parietal bone	rgb(229,204,109)	
145	right temporal bone	rgb(255,243,152)	
146	left temporal bone	rgb(255,243,152)	
147	right sphenoid bone	rgb(209,185,85)	
148	left sphenoid bone	rgb(209,185,85)	
149	right ethmoid bone	rgb(248,223,131)	
150	left ethmoid bone	rgb(248,223,131)	
151	occipital bone	rgb(255,230,138)	
152	maxilla	rgb(196,172,68)	
153	right zygomatic bone	rgb(255,255,167)	
154	right lacrimal bone	rgb(255,250,160)	
155	vomer bone	rgb(255,237,145)	
156	right palatine bone	rgb(242,217,123)	
157	left palatine bone	rgb(242,217,123)	
158	mandible	rgb(222,198,101)	

159	neck	rgb(177,122,101)	
160	muscles of neck	rgb(213,124,109)	
161	pharynx	rgb(184,105,108)	
162	larynx	rgb(150,208,243)	
163	thyroid gland	rgb(62,162,114)	
164	right parathyroid glands	rgb(62,162,114)	
165	left parathyroid glands	rgb(62,162,114)	
166	skeleton of neck	rgb(242,206,142)	
167	hyoid bone	rgb(250,210,139)	
168	cervical vertebral column	rgb(255,255,207)	
169	thorax	rgb(177,122,101)	
170	trachea	rgb(182,228,255)	
171	bronchi	rgb(175,216,244)	
172	right lung	rgb(197,165,145)	
173	left lung	rgb(197,165,145)	
174	superior lobe of right lung	rgb(172,138,115)	
175	superior lobe of left lung	rgb(172,138,115)	
176	middle lobe of right lung	rgb(202,164,140)	
177	inferior lobe of right lung	rgb(224,186,162)	
178	inferior lobe of left lung	rgb(224,186,162)	
179	pleura	rgb(255,245,217)	
180	heart	rgb(206,110,84)	
181	right atrium	rgb(210,115,89)	
182	left atrium	rgb(203,108,81)	
183	atrial septum	rgb(233,138,112)	
184	ventricular septum	rgb(195,100,73)	
185	right ventricle of heart	rgb(181,85,57)	
186	left ventricle of heart	rgb(152,55,13)	

187	mitral valve	rgb(159,63,27)	
188	tricuspid valve	rgb(166,70,38)	
189	aortic valve	rgb(218,123,97)	
190	pulmonary valve	rgb(225,130,104)	
191	aorta	rgb(224,97,76)	
192	pericardium	rgb(255,244,209)	
193	pericardial cavity	rgb(184,122,154)	
194	esophagus	rgb(211,171,143)	
195	thymus	rgb(47,150,103)	
196	mediastinum	rgb(255,244,209)	
197	skin of thoracic wall	rgb(173,121,88)	
198	muscles of thoracic wall	rgb(188,95,76)	
199	skeleton of thorax	rgb(255,239,172)	
200	thoracic vertebral column	rgb(226,202,134)	
201	ribs	rgb(253,232,158)	
202	sternum	rgb(244,217,154)	
203	right clavicle	rgb(205,179,108)	
204	left clavicle	rgb(205,179,108)	
205	abdominal cavity	rgb(186,124,161)	
206	abdomen	rgb(177,122,101)	
207	peritoneum	rgb(255,255,220)	
208	omentum	rgb(234,234,194)	
209	peritoneal cavity	rgb(204,142,178)	
210	retroperitoneal space	rgb(180,119,153)	
211	stomach	rgb(216,132,105)	
212	duodenum	rgb(255,253,229)	
213	small bowel	rgb(205,167,142)	
214	colon	rgb(204,168,143)	

215	anus	rgb(255,224,199)	
216	liver	rgb(221,130,101)	
217	biliary tree	rgb(0,145,30)	
218	gallbladder	rgb(139,150,98)	
219	pancreas	rgb(249,180,111)	
220	spleen	rgb(157,108,162)	
221	urinary system	rgb(203,136,116)	
222	right kidney	rgb(185,102,83)	
223	left kidney	rgb(185,102,83)	
224	right ureter	rgb(247,182,164)	
225	left ureter	rgb(247,182,164)	
226	urinary bladder	rgb(222,154,132)	
227	urethra	rgb(124,186,223)	
228	right adrenal gland	rgb(249,186,150)	
229	left adrenal gland	rgb(249,186,150)	
230	female internal genitalia	rgb(244,170,147)	
231	uterus	rgb(255,181,158)	
232	right fallopian tube	rgb(255,190,165)	
233	left fallopian tube	rgb(227,153,130)	
234	right ovary	rgb(213,141,113)	
235	left ovary	rgb(213,141,113)	
236	vagina	rgb(193,123,103)	
237	male internal genitalia	rgb(216,146,127)	
238	prostate	rgb(230,158,140)	
239	right seminal vesicle	rgb(245,172,147)	
240	left seminal vesicle	rgb(245,172,147)	
241	right deferent duct	rgb(241,172,151)	
242	left deferent duct	rgb(241,172,151)	
243	skin of abdominal wall	rgb(177,124,92)	

244	muscles of abdominal wall	rgb(171,85,68)	
245	skeleton of abdomen	rgb(217,198,131)	
246	lumbar vertebral column	rgb(212,188,102)	
247	female external genitalia	rgb(185,135,134)	
248	male external genitalia	rgb(185,135,134)	
249	skeleton of upper limb	rgb(198,175,125)	
250	muscles of upper limb	rgb(194,98,79)	
251	right upper limb	rgb(177,122,101)	
252	left upper limb	rgb(177,122,101)	
253	right shoulder	rgb(177,122,101)	
254	left shoulder	rgb(177,122,101)	
255	right arm	rgb(177,122,101)	
256	left arm	rgb(177,122,101)	
257	right elbow	rgb(177,122,101)	
258	left elbow	rgb(177,122,101)	
259	right forearm	rgb(177,122,101)	
260	left forearm	rgb(177,122,101)	
261	right wrist	rgb(177,122,101)	
262	left wrist	rgb(177,122,101)	
263	right hand	rgb(177,122,101)	
264	left hand	rgb(177,122,101)	
265	skeleton of lower limb	rgb(255,238,170)	
266	muscles of lower limb	rgb(206,111,93)	
267	right lower limb	rgb(177,122,101)	
268	left lower limb	rgb(177,122,101)	
269	right hip	rgb(177,122,101)	
270	left hip	rgb(177,122,101)	
271	right thigh	rgb(177,122,101)	

272	left thigh	rgb(177,122,101)	
273	right knee	rgb(177,122,101)	
274	left knee	rgb(177,122,101)	
275	right leg	rgb(177,122,101)	
276	left leg	rgb(177,122,101)	
277	right foot	rgb(177,122,101)	
278	left foot	rgb(177,122,101)	
279	peripheral nervous system	rgb(216,186,0)	
280	autonomic nerve	rgb(255,226,77)	
281	sympathetic trunk	rgb(255,243,106)	
282	cranial nerves	rgb(255,234,92)	
283	vagus nerve	rgb(240,210,35)	
284	peripheral nerve	rgb(224,194,0)	
285	circulatory system	rgb(213,99,79)	
286	systemic arterial system	rgb(217,102,81)	
287	systemic venous system	rgb(0,147,202)	
288	pulmonary arterial system	rgb(0,122,171)	
289	pulmonary venous system	rgb(186,77,64)	
290	lymphatic system	rgb(111,197,131)	
291	needle	rgb(240,255,30)	
292	region 0	rgb(185,232,61)	
293	region 1	rgb(0,226,255)	
294	region 2	rgb(251,159,255)	
295	region 3	rgb(230,169,29)	
296	region 4	rgb(0,194,113)	
297	region 5	rgb(104,160,249)	
298	region 6	rgb(221,108,158)	

299	region 7	rgb(137,142,0)	
300	region 8	rgb(230,70,0)	
301	region 9	rgb(0,147,0)	
302	region 10	rgb(0,147,248)	
303	region 11	rgb(231,0,206)	
304	region 12	rgb(129,78,0)	
305	region 13	rgb(0,116,0)	
306	region 14	rgb(0,0,255)	
307	region 15	rgb(157,0,0)	
308	unknown	rgb(100,100,130)	
309	cyst	rgb(205,205,100)	